Study of Soot Growth and Nucleation by a Time-Resolved Synchrotron Radiation Based X-Ray Absorption Method

Final Report on EOARD Contract No: F61775-00-WE039

J. Brian A. MITCHELL

Physique des Atomes, Lasers, Molécules et Surfaces (P.A.L.M.S.)

U.M.R. du C.N.R.S. No. 6627

Université de Rennes I

35042 Rennes, France

5 July 2001

Form SF298 Citation Data

Report Date *("DD MON YYYY")* 05072001	**Report Type** Final	**Dates Covered (from... to)** *("DD MON YYYY")*

Title and Subtitle Study Of Soot Growth And Nucleation By A Time-Resolved Synchrotron Radiation Based X-Ray Absorption Method	**Contract or Grant Number** F61775-00-WE039
	Program Element Number
Authors Mitchell, J. Brian A.	**Project Number**
	Task Number
	Work Unit Number
Performing Organization Name(s) and Address(es) University of Rennes I Campus de Beaulieu Rennes 35042 France	**Performing Organization Number(s)**
Sponsoring/Monitoring Agency Name(s) and Address(es) EOARD PSC 802 BOX 14 FPO 09499-0200	**Monitoring Agency Acronym**
	Monitoring Agency Report Number(s)
Distribution/Availability Statement Approved for public release, distribution unlimited	
Supplementary Notes	

Abstract

This report results from a contract tasking University of Rennes I as follows: The contractor will perform a study of soot growth and nucleation by a time-resolved synchrotron radiation based x-ray absorption method. A gaseous fuel burner will be constructed that will allow a stable flame to be produced. The burner will be mounted on an assembly that will allow the motorized movement in both a horizontal and vertical direction so that the two dimensional profile of the soot density can be measured via x-ray absorption. Associated fuel flow control equipment will be used to control and characterize flame conditions. The goal of this work therefore will be to (a) determine doped and undoped soot particle photoemission yields (b) map out the soot density structure in a heavily sooting flame using x-ray absorption and photoelectron detection and (c) determine the influence of enhanced ionization on subsequent soot growth in flames.

Subject Terms

EOARD; Combustion; Soot Formation

Document Classification unclassified	**Classification of SF298** unclassified

Classification of Abstract unclassified	**Limitation of Abstract** unlimited
Number of Pages 35	

REPORT DOCUMENTATION PAGE

Form Approved OMB No. 0704-0188

1. AGENCY USE ONLY (Leave blank)	2. REPORT DATE	3. REPORT TYPE AND DATES COVERED
	05-July-2001	Final Report

4. TITLE AND SUBTITLE

Study Of Soot Growth And Nucleation By A Time-Resolved Synchrotron Radiation Based X-Ray Absorption Method

5. FUNDING NUMBERS

F61775-00-WE039

6. AUTHOR(S)

Professor J. Brian A. Mitchell

7. PERFORMING ORGANIZATION NAME(S) AND ADDRESS(ES)

University of Rennes I
Campus de Beaulieu
Rennes 35042
France

8. PERFORMING ORGANIZATION REPORT NUMBER

N/A

9. SPONSORING/MONITORING AGENCY NAME(S) AND ADDRESS(ES)

EOARD
PSC 802 BOX 14
FPO 09499-0200

10. SPONSORING/MONITORING AGENCY REPORT NUMBER

SPC 00-4039

11. SUPPLEMENTARY NOTES

12a. DISTRIBUTION/AVAILABILITY STATEMENT

Approved for public release; distribution is unlimited.

12b. DISTRIBUTION CODE

A

13. ABSTRACT (Maximum 200 words)

This report results from a contract tasking University of Rennes I as follows: The contractor will perform a 'study of soot growth and nucleation by a time-resolved synchrotron radiation based x-ray absorption method'. A gaseous fuel burner will be constructed that will allow a stable flame to be produced. The burner will be mounted on an assembly that will allow the motorized movement in both a horizontal and vertical direction so that the two dimensional profile of the soot density can be measured via x-ray absorption. Associated fuel flow control equipment will be used to control and characterize flame conditions.
The goal of this work therefore will be to (a) determine doped and undoped soot particle photoemission yields (b) map out the soot density structure in a heavily sooting flame using x-ray absorption and photoelectron detection and (c) determine the influence of enhanced ionization on subsequent soot growth in flames.

14. SUBJECT TERMS

EOARD, Combustion, Soot Formation

15. NUMBER OF PAGES

35

16. PRICE CODE

N/A

17. SECURITY CLASSIFICATION OF REPORT	18. SECURITY CLASSIFICATION OF THIS PAGE	19, SECURITY CLASSIFICATION OF ABSTRACT	20. LIMITATION OF ABSTRACT
UNCLASSIFIED	UNCLASSIFIED	UNCLASSIFIED	UL

DECLARATIONS

The Contractor, University of Rennes I, hereby declares that, to the best of its knowledge and belief, the technical data delivered herewith under Contract No. F61775-00-WE039 is complete, accurate, and complies with all requirements of the contract.

DATE : 6 July 2001

Professor J. Brian A. MITCHELL

I certify that there were no subject inventions to declare in FAR 52.227-13, during the performance of this contract

DATE : 6 July 2001

Professor J. Brian A. MITCHELL

1. Introduction

The formation of soot particles in a flame is still a subject that is not well understood. It is nevertheless a very important subject for soot not only produces visible obscurity in large fires but it represents a serious pollution emission. Young soot particles that form during the combustion process, manifest themselves by producing the yellow-orange emission, characteristic of hydrocarbon flames. They have diameters ranging from a few to tens of nanometers.

Soot is formed during the combustion of hydrocarbon fuels though if there is sufficient air present, the soot particles are oxidized and thus destroyed during the combustion process. If there is insufficient oxygen, the particles will survive passage through the reaction zone of the flame and be emitted into the surrounding air in the form of visible smoke. This represents not only an unsightly but a dangerous pollutant emission. Soot particles contain condensed polycyclic aromatic hydrocarbon (PAH) species, many of which are known carcinogens and since they can have sub-micron diameters, they can pass through the bronchial canals and deposit in the lungs of individuals so exposed. From an engineering standpoint, soot also plays an important role in the radiative transfer of thermal energy and thus its production is important for the thermal efficiency of engines and boilers

The formation of soot particles begins with the thermal pyrolysis of the fuel to form radical fragments that react rapidly with oxidant species such as O_2 , O and OH and with hydrocarbon radicals. A chain of radical-molecule reactions ensues that results in the formation of large soot precursor molecules that act as nucleation sites for the growth of

particulates via the condensation and surface reaction of molecules and radicals and via agglomeration processes where colliding particulates stick together or coalesce. In this phase of the process, the particles can be solid or liquid in form. As the particles age though, they lose hydrogen and thus mature soot particles have an almost graphitic structure. The timescale for the process is of the order of a few milliseconds and this renders its study difficult, particularly with regard to the early phases prior to nucleation and solid particle formation.

A number of different techniques have been developed to map the presence of soot particles in a flame, to determine their number density, their size distribution, their geometric form, and their chemical composition. Non-intrusive techniques include visible light absorption [1], the Rayleigh scattering of visible light [2], depolarization measurements [2], laser induced incandescence [3], laser induced emission [4], UV absorption and fluorescence [5], laser ionization [6] and multiwavelength analysis of soot radiation [7]. Intrusive methods involve the physical extraction of soot particles from flames by for example, thermophoretic sampling [8]. The particles are subsequently analyzed by techniques such as particle mobility analysis [9], scanning electron microscopy [10], transmission electron microscopy [11-13], laser microprobe mass spectrometry [14], laser desorption mass spectrometry [15] and real time mass spectrometry [16]. Other techniques such as flame sampling mass spectrometry [17] and laser induced fluorescence [18] are used to identify soot precursors and primary reactants in the soot formation process. All of these techniques have their individual strengths and weaknesses and the information gleaned from their use has served to provide a series of snapshots in the life-span of soot particles in a flame. This has provided us with an overview of the physical and chemical development of soot.

This subject of in-situ nanoparticle identification and analysis is not limited to classical combustion processes but is also important for the analysis of flames that are used for the formation of nano-particulate forms of compounds such as TiO_2 and SiO_2 [19,20]. Soot-like nanoparticles are believed to exist in the interstellar medium and knowledge of their formation and interaction with the intense photon and particle fluxes emanating from hot stars is important for astrophysical modeling [21-26]. Silicon and carbon based nanoparticles are formed in plasma used for semiconductor and materials processing and for pollutant destruction.

While the non-intrusive methods listed above have been invaluable for the analysis of small laboratory scale flames under lightly sooting conditions, they run into serious problems when the particle density rises to the point where self re-absorption of scattered or emitted light becomes significant. They are cumbersome to use therefore under heavy particulate loading conditions or where the size of the combustion system becomes large. In the latter case, the intrusive methods become equally difficult to apply.

The purpose of this report is to present the first results from an alternative flame sampling method that uses x-rays to probe soot particles. The method is based upon detecting the charged species formed from the ionization of soot nanoparticles by x-ray absorption, a process commonly refered to as *photoemission*. High energy X-rays are very penetrating due to their weak interaction with matter and thus the problems associated with absorption or re-absorption of visible or ultraviolet light can be avoided. This weak interaction makes it difficult to use scattering or transmission methods for assessing the presence of soot particles but the high efficiency with which charged particles can be detected renders the technique

feasible. Indeed in the experiment described below, detection of the ionization currents was achieved with the use of a simple electrically biased wire probe.

2. Experimental Method

The basic apparatus used for this experiment consists of a cylindrically symmetric burner (11 mm diameter) through which the fuel gas passes. The burner is surrounded by a 100 mm diameter chimney. Air from a compressor is fed into the base of the chimney and passes through a series of wire meshes, between which are placed layers of glass beads, 1 mm in diameter. This allows a laminar curtain of air to surround the burner, thus producing a stable diffusion flame. (In a diffusion flame, the surrounding air diffuses into the fuel flow in order to produce the combustion reaction. The actual reacting surface is very thin and conical in form). Flow rates for the fuel gas and for the air are controlled and metered using rotameters. In most of the experiments described in this report, a fixed fuel flow rate of 62 ml/min and an air flow rate of 39l/min were used The burner has an overall height of 100 mm and the chimney, of 500 mm. At the top of the chimney, a cap is placed that can be fitted with a glass fiber filter to collect soot particles. Combustion gases are drawn through a hole in the cap by means of an aspirating pump. The position of the cap is variable with respect to the burner mouth and the pump line can be fitted with a collection trap. In some experiments, this trap was immersed in water to cool the exhaust gases prior to entering the pump. The overall assembly is illustrated in figure 1.

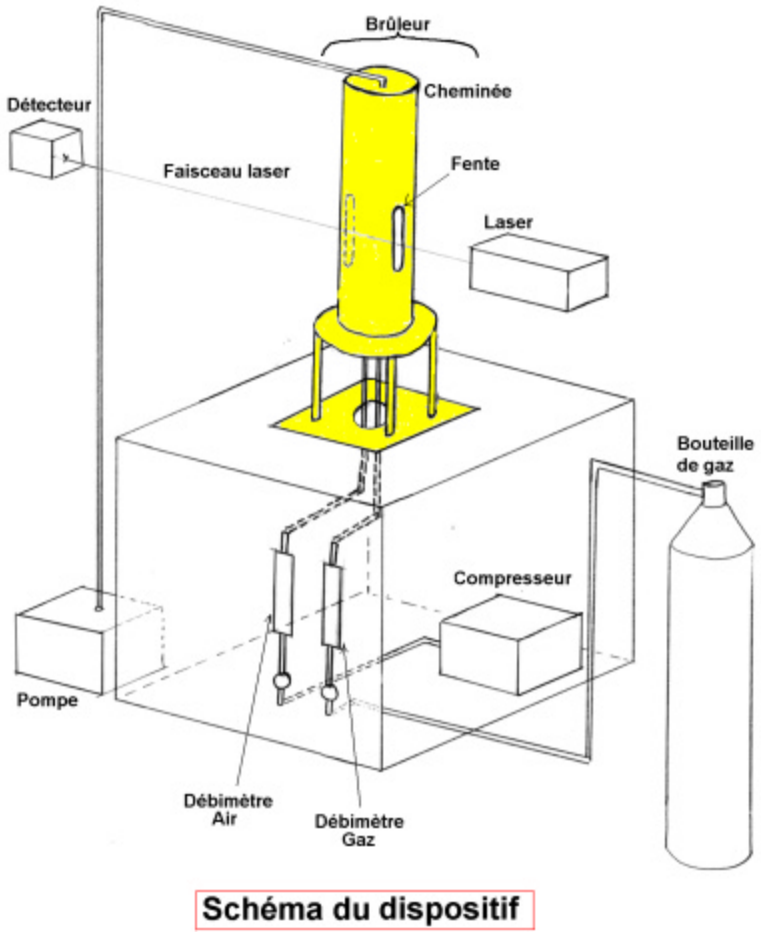

Figure 1. Schematic of the burner assembly at the University of Rennes showing the gas feed system.

The burner and chimney assembly are mounted on two plates as shown in figure 2. The upper plate can be moved with respect to the lower thus allowing the flame to be moved vertically with respect to a stationary probe or a sampling beam from a laser or from a synchrotron beamline. The lower plate can be moved horizontally thus allowing the flame to be moved horizontally with respect to a stationary probe or sampling beam. This assembly allows Y-Z scans to be made of the flame (X being the direction of the sampling beam) and thus the position of flame components can be mapped. In this apparatus, the flame is cylindrically symmetric and this allows the radial profiles of flame components to be determined by means of tomographic re-construction which is discussed later in the report.

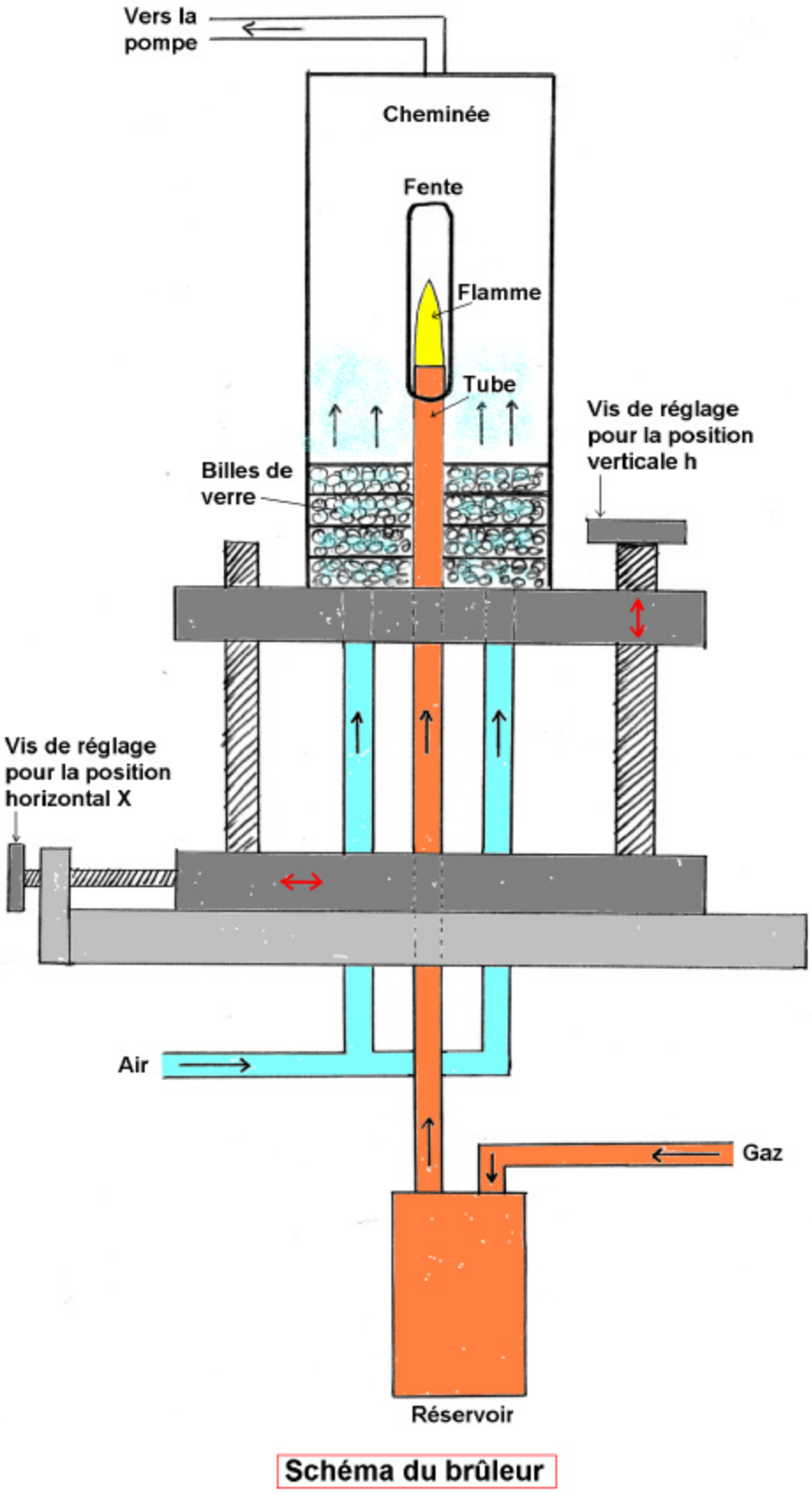

Figure 2. Schematic of the burner at the University of Rennes showing the Y and Z translation stages. The reservoir is heated and can be used to inject ferrocene vapor into the fuel stream.

Three types of experiments have been performed including mapping measurements of He/Ne laser absorption, of charged species naturally present in the flame and of the absorption of an x-ray beam from a synchrotron radiation facility. The latter experiment is believed to be the first of its kind and opens up an entirely new field of research, namely the study of the interaction of x-rays with nano-particles. Each experiment and the individual experimental set-ups are discussed in the following sections.

3. Experimental Results

3.1 Laser Absorption Experiments.

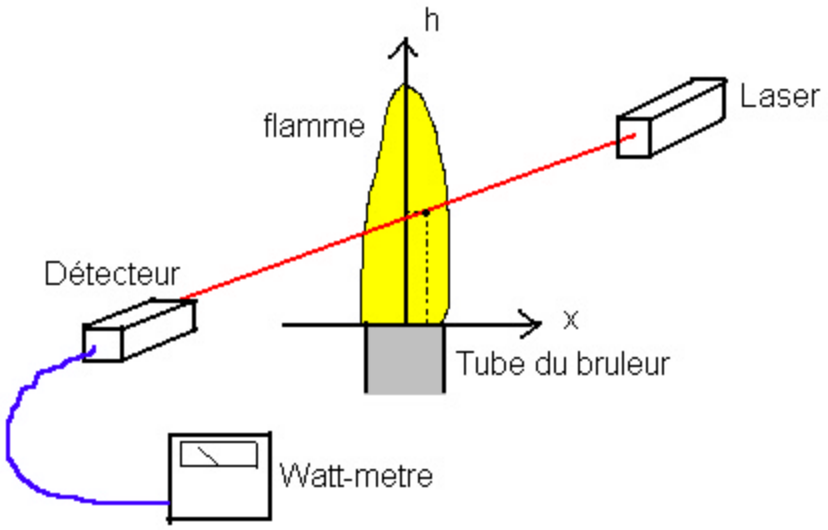

Figure 3. Sketch of the arrangement used for the laser absorption experiment.

The basic set-up for this experiment is illustrated in figure 3. The measurement involves the use of a power meter to detect light from a helium/neon laser that is scanned across the flame. The amount of absorption by soot particles in the flame is determined as a function of position in the flame. The ratio of the transmitted intensity I to the initial intensity I_0 of the laser beam yields the *soot volume fraction*[1] f_v in the flame via the formula:

[1] Soot volume fraction is defined as the fractional volume of the flame occupied by soot particles.

$$f_v = \frac{l}{KL} \ln\left(\frac{I}{I_0}\right) \ldots.(1)$$

where λ = 632.8 nm is the wavelength of the laser light

K=4.9 is the absorption constant for soot particles at this wavelength [1].

L is the optical depth of the flame at the given height and radius at which the measurement is taken.

This experiment is very simple in nature and the results thus obtained are shown in figure 4, where f_v is plotted as a function of *h*, the height above the burner mouth. It can be seen that low down in the flame, the soot is concentrated mostly in an annular ring while higher up, the soot particles are concentrated near the center of the flame. This distribution is illustrated in a false color contour chart in figure 5 and in fact this very much resembles what one sees with the naked eye while looking at the flame. Soot forms at the edges of the flame where the reaction between the fuel and air occurs and as one moves up, this region shrinks in diameter eventually forming a continuous zone. Higher up still, the soot density decreases as the soot particles become oxidized. In the flame shown here, there was no emission of visible smoke indicating that the soot density had dropped to a low level. The overall flame height was 50 mm and the fuel and air flow rates used in this case were 84 ml/min and 39 l/min respectively.

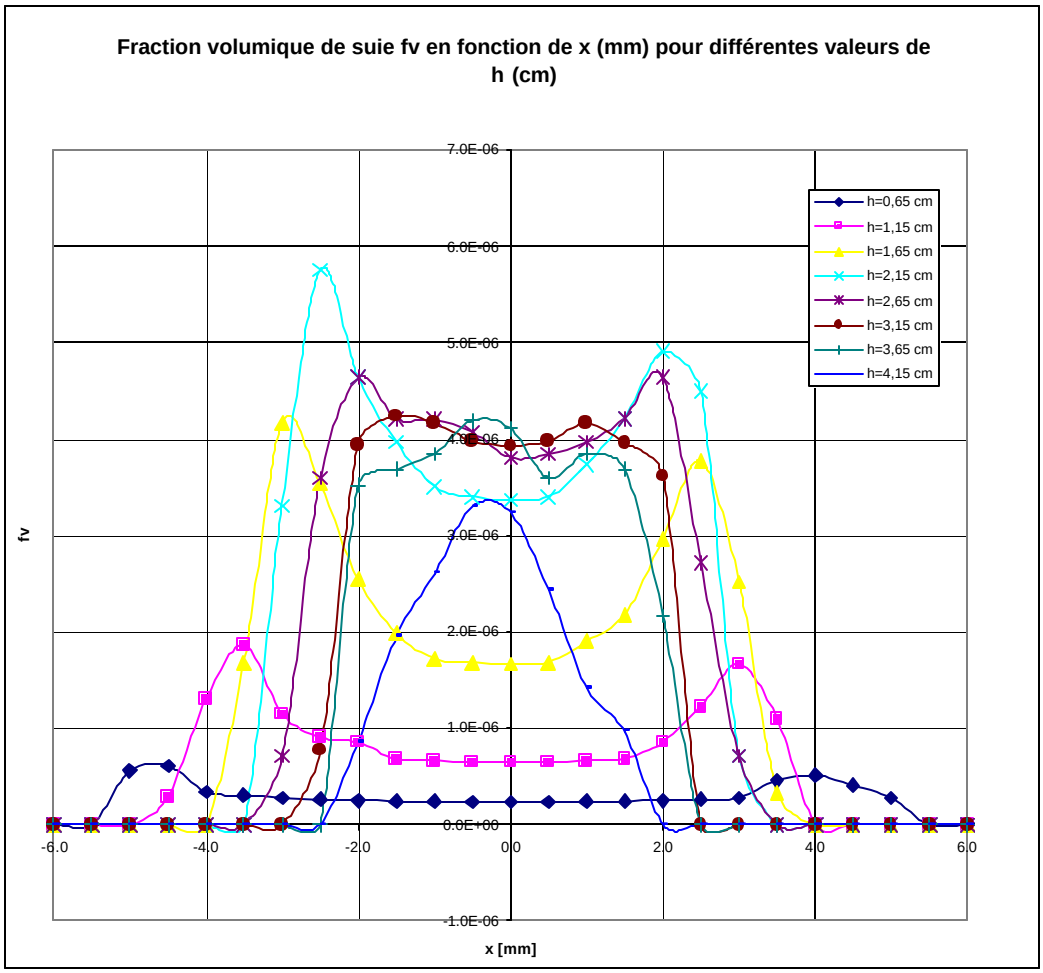
Fraction volumique de suie fv en fonction de x (mm) pour différentes valeurs de h (cm)
fv
x [mm]
7.0E-06
6.0E-06
5.0E-06
4.0E-06
3.0E-06
2.0E-06
1.0E-06
0.0E+00
-1.0E-06
-6.0
-4.0
-2.0
0.0
2.0
4.0
6.0
h=0,65 cm
h=1,15 cm
h=1,65 cm
h=2,15 cm
h=2,65 cm
h=3,15 cm
h=3,65 cm
h=4,15 cm

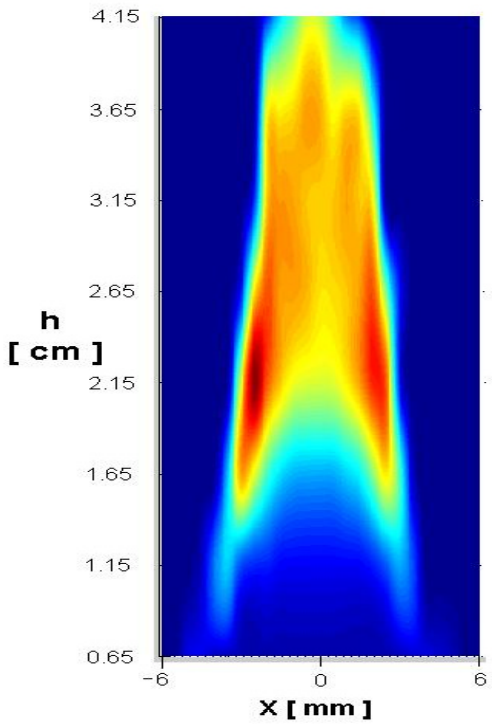
4.15
3.65
3.15
2.65
2.15
1.65
1.15
0.65
h
[cm]
-6
0
6
X [mm]

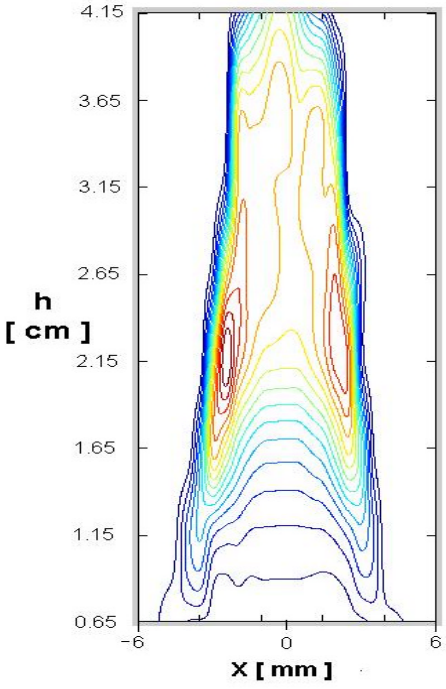
4.15
3.65
3.15
2.65
2.15
1.65
1.15
0.65
h
[cm]
-6
0
6
X [mm]

Graph 1

Figure 5. False color contour plots of the soot volume fraction (uncorrected)

Figure 4 actually needs correction in order that the true radial distribution of soot volume fraction can be determined. The data shown is obtained from the transmitted laser intensity but the laser passes through regions of varying soot density. This can be corrected for using a tomographic re-construction technique [27, 28] and the resulting distribution of soot volume fraction is shown in figure 6.

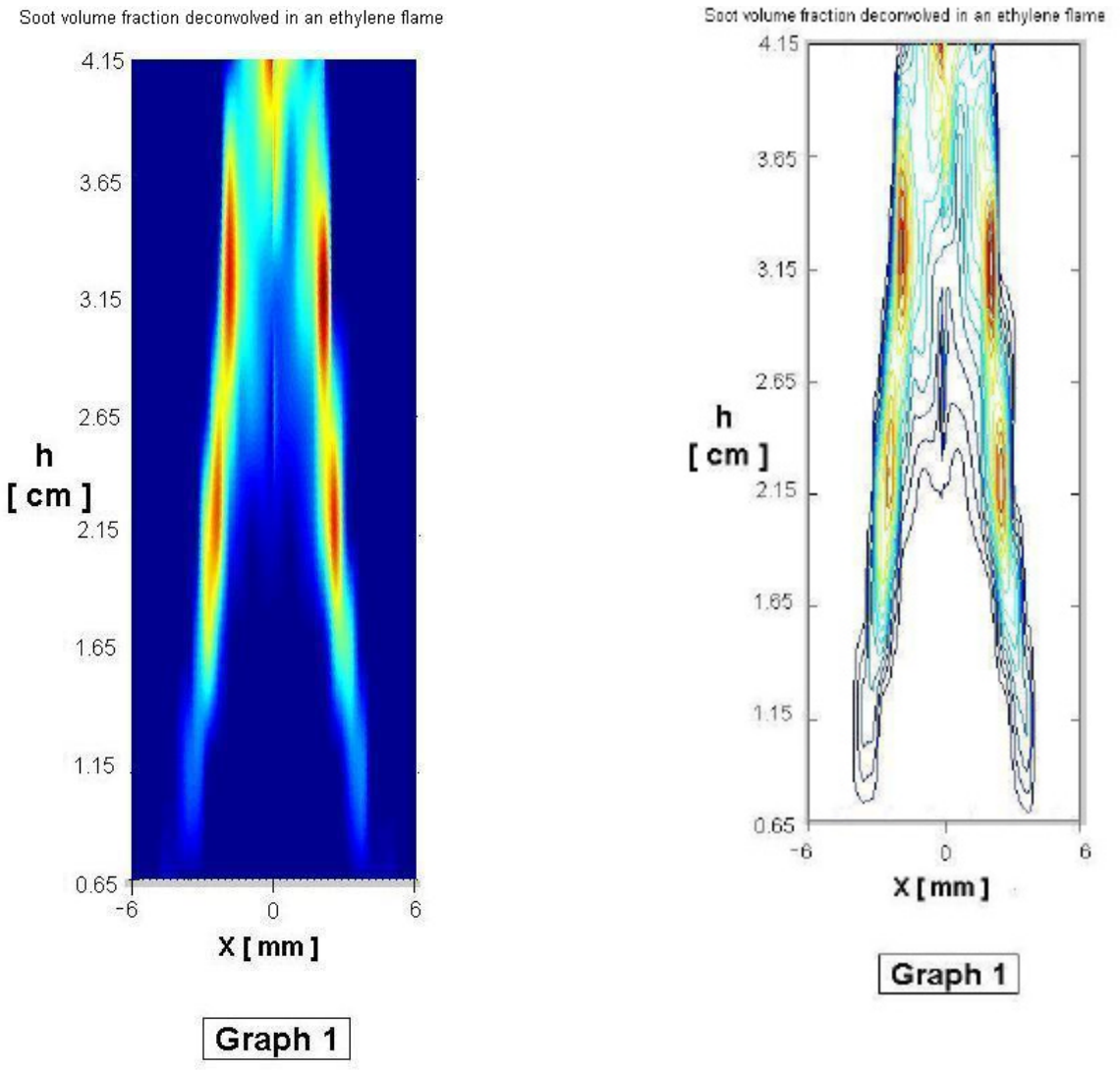

Fig. 6. Contour plots of flame following tomographic reconstruction.

3.2 Natural Flame Charge Distribution Measurement

Most hydrocarbon flames contain ions, electrons and charged particulates that are formed via a number of processes. The associative ionization reaction:

$$CH + O \rightarrow CHO^{+} + e$$

has been identified as the origin of ionization in air rich flames while the reaction:

$$CH + C_2H_2 \rightarrow C_3H_3^{+} + e$$

dominates in fuel rich flames where soot particles are formed. These ions react with other neutral soot species to form other ions which in turn are eventually neutralized through dissociative recombination reactions such as:

$$C_xH_y^{+} + e \rightarrow C_xH_{y-1} + H$$

Extensive mapping of natural flame ions has been performed for pre-mixed flames by a number of workers using both ion-sampling mass spectrometers [29-33] and Langmuir Probes [34] and it is found that densities of most ions fall off rapidly a few millimeters above the burner mouth although some heavier species can be found at 20 mm above the burner mouth.

Higher up in the flame, charged soot particles are found and these acquire their charge either by thermionic emission of electrons or via electron attachment processes. Generally the former process seems to be more effective as positive soot charges tend to dominate.

As part of a self consistent measurement program, the charge particle distribution in our ethylene flame was measured by scanning a 1 mm diameter, 6 cm long cylindrical electrode radially across the flame for a series of different heights. With the electrode biased positively,

mainly electrons (with probably some negative ions and soot particles) are detected while a negatively biased probe will sample positive ions and particles.

The results so obtained are illustrated in figure 7. It is seen that just above the burner mouth, the distribution of both positive and negative species is structured while further up the distributions become more uniform.

This data serves as a reference for the measurements described in the next section

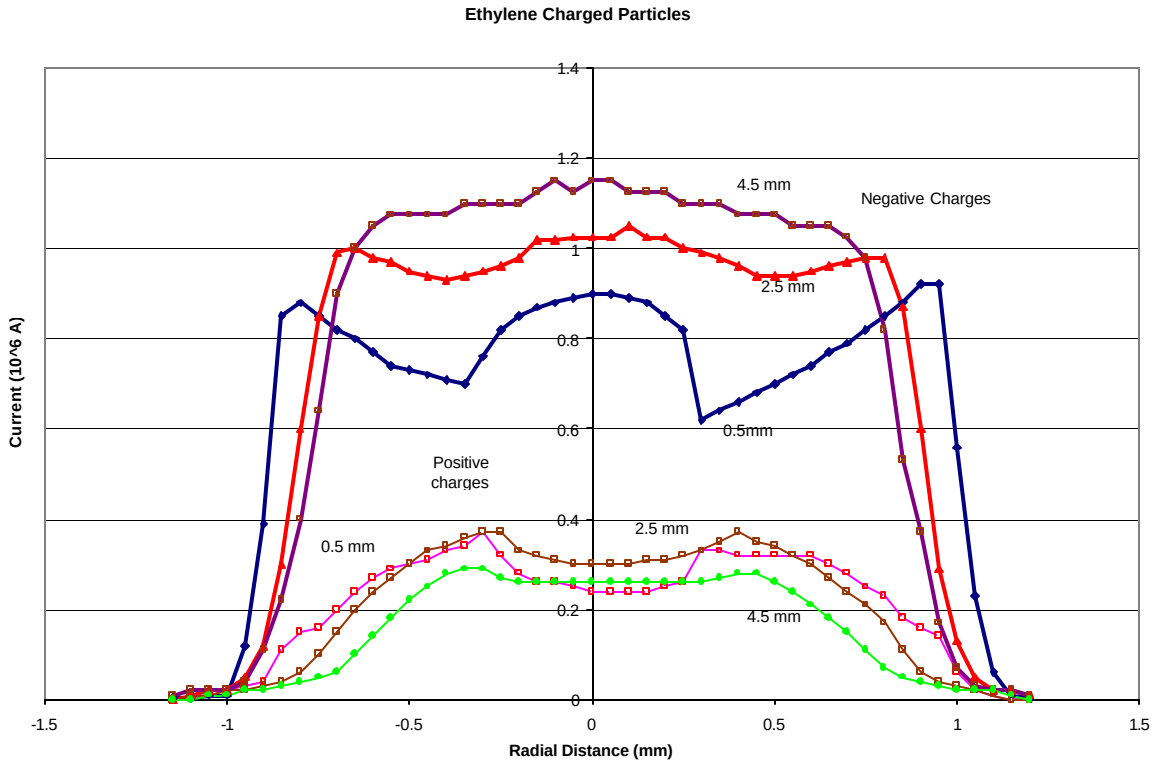

Fig. 7a: Charged species measured as a function of height and radial distance

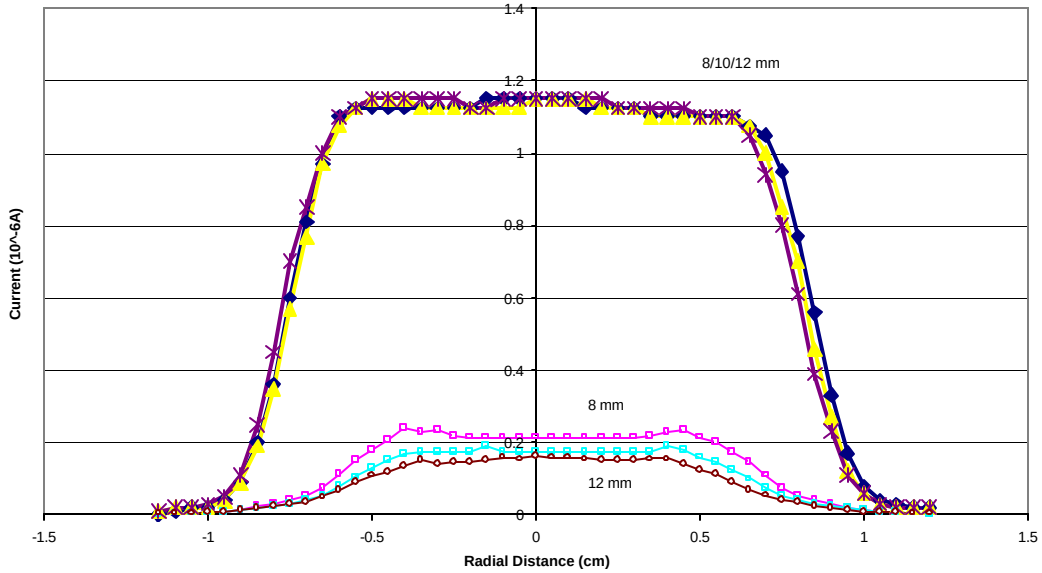

Fig. 7b. Heights 8 mm, 10 mm, 12 mm.

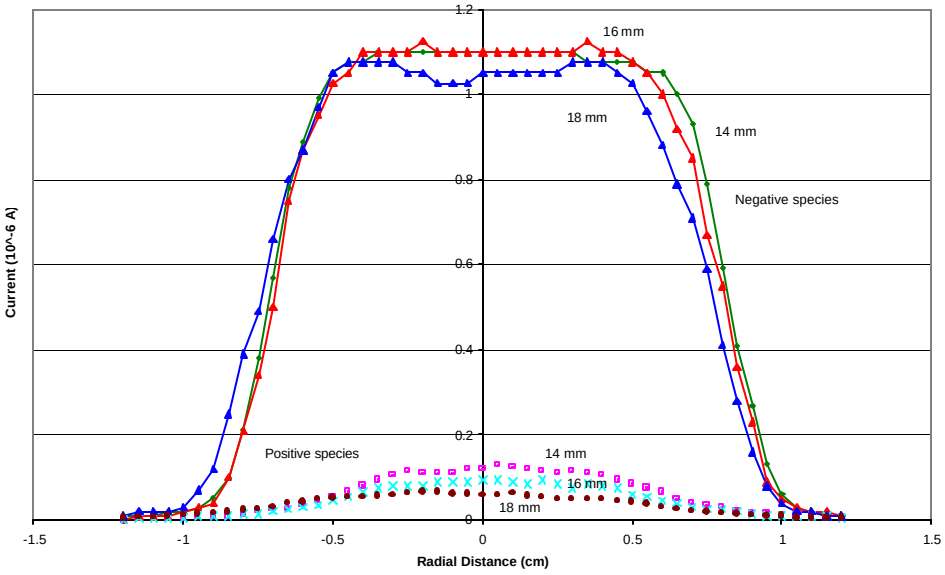

Fig. 7c. Heights 14 mm, 16 mm, 18 mm

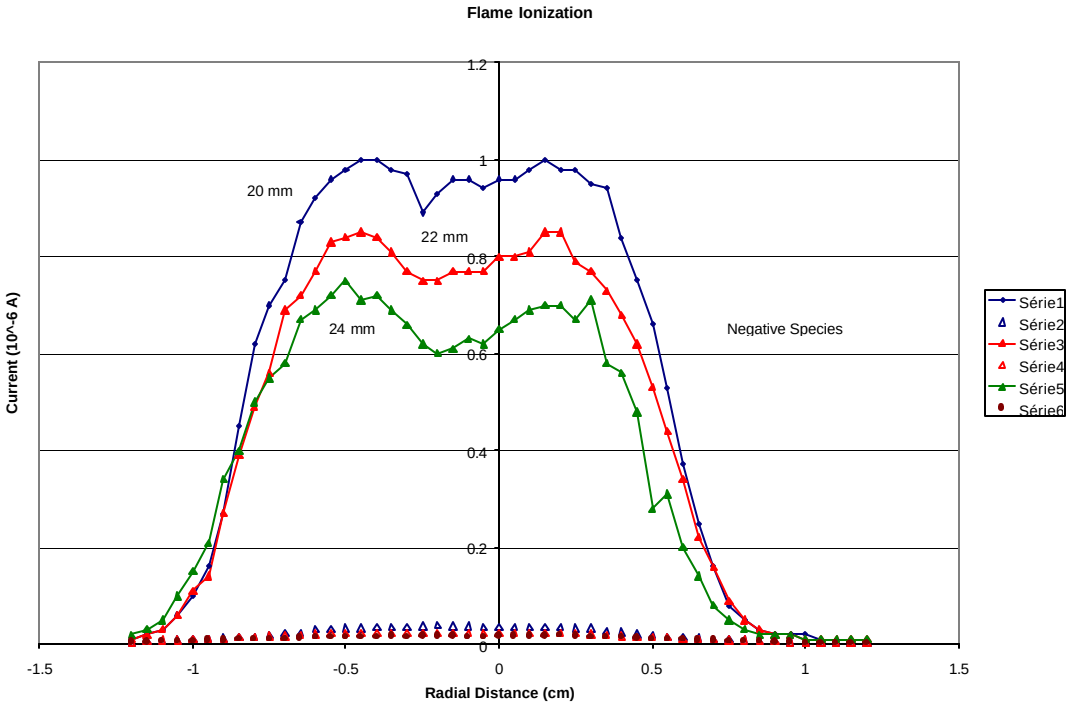

Fig. 7d. Heights 20 mm, 22 mm, 24 mm.

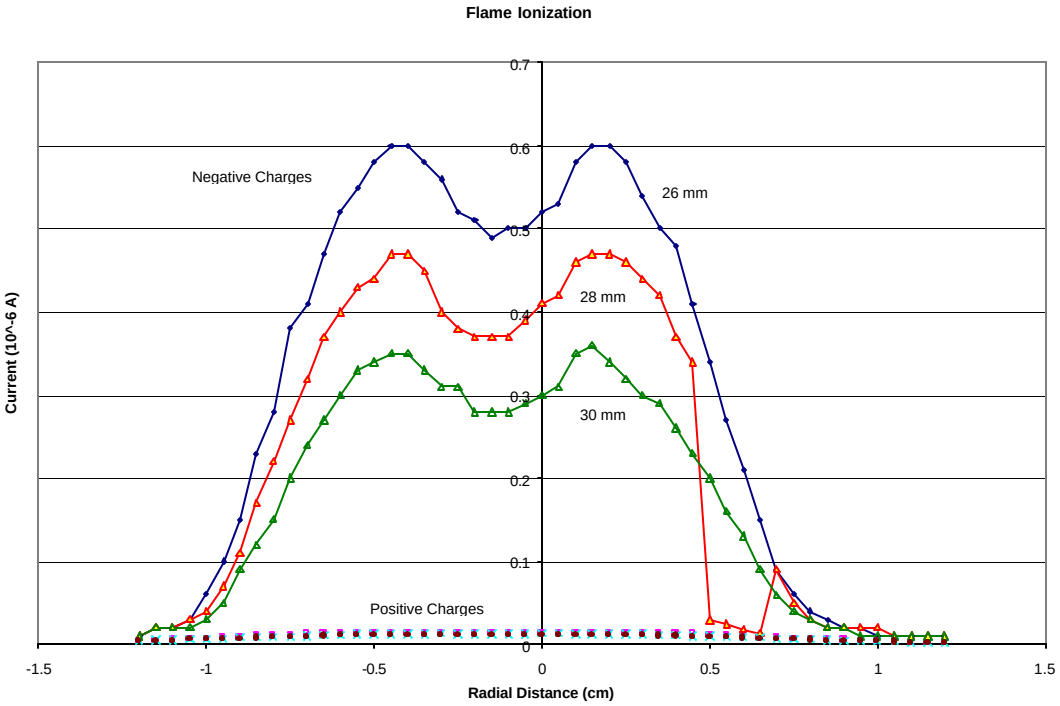

Fig. 7 e. Heights 26 mm, 28 mm, 30 mm.

3.3 X-Ray Absorption Measurements

This is the main part of the experimental work that has been carried out concerning the mapping of soot particles in an ethylene flame. The basic idea behind the experiment was to pass an x-ray beam from a synchrotron radiation beamline through the ethylene flame and to detect any ionization produced by absorption by soot particles, using a biased wire probe.

The experiment was carried out on the ID09 white beam undulator beamline at the European Synchrotron Radiation Facility (ESRF) in Grenoble, France. A 6 GeV electron beam is magnetically stored in a ring structure and each time it is deviated by a magnet, it emits electromagnetic radiation over a very wide wavelength range. The ID09 beam line accepts x-rays generated by an undulator device, located in one of the straight sections of the electron ring. In the undulator, the electron beam is made to undulate periodically by an array of oppositely polarized magnets, thus emitting electromagnetic radiation coherently at each deviation. Much higher photon intensities are made possible by the use of the undulator though the wavelength range thus obtained is much narrower than emitted by a conventional bending magnet. In the front end of the ID09 beamline, a monochromator can be used to energy select the photons arriving into the line but in the present experiment, a white beam arriving directly from the undulator was used. The photon flux was 3×10^{11} photons/sec and the beam dimensions at the flame were 50μm x 50μm. The x-rays in the beam ranges in energy from 5 to 35 keV. A white beam was used in order to provide a good signal strength in this proof-of-principal experiment although in fact a much more intense beam could have been obtained by opening up the collimation slits. It was found that this was not necessary and so narrow slits were used to avoid ozone production in the experimental hutch, caused by the passage of the beam through the air. Figure 8 shows a sketch of the beamline.

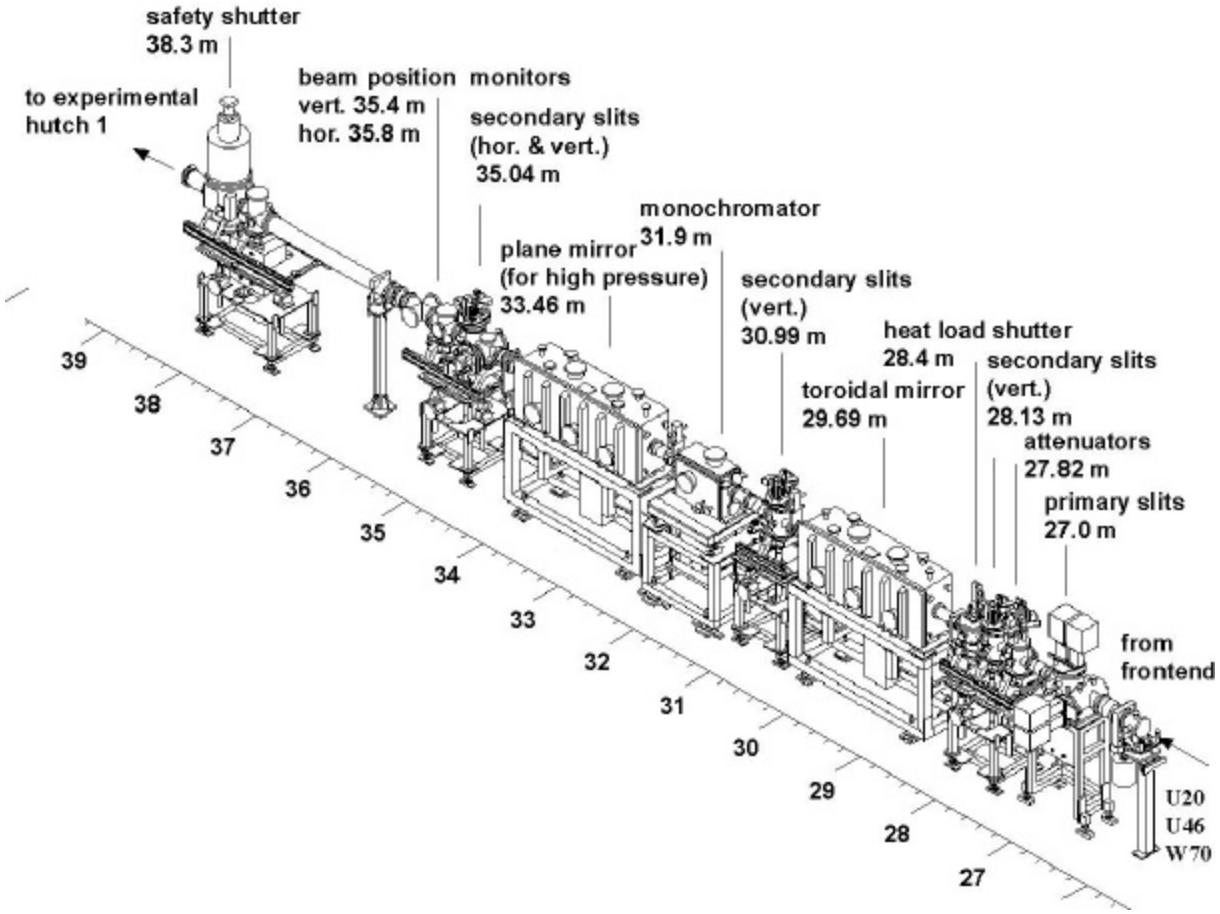

Fig. 8 Diagram of the optics section of the ID09 beamline.

At the end of the beamline, the x-rays pass through a cylindrical pipe and on into the air. The whole assembly is housed in a lead-lined experimental hutch fitted with elaborate safety interlocks. It is not possible to be present in the hutch when the beam is operational for safety reasons. The beam can be switched on and off using a beam shutter.

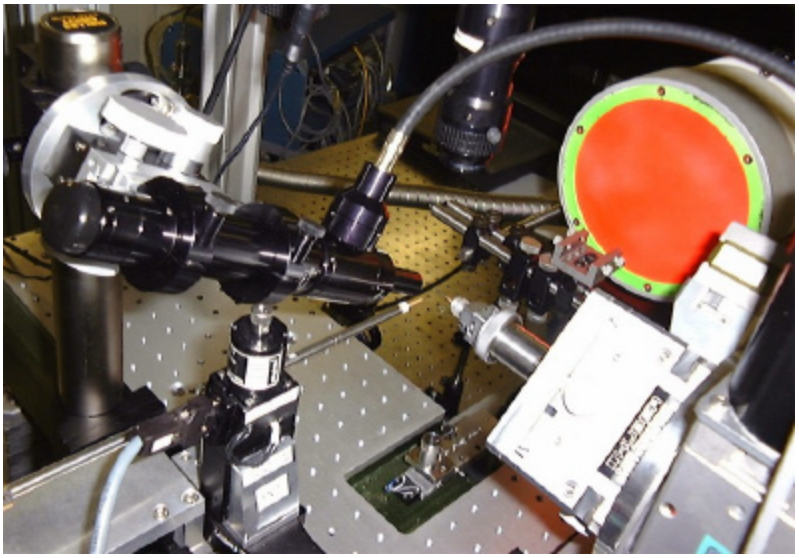

Fig. 9. This photograph shows the beam pipe (coming from the bottom left) and in front of it (with the orange cover) is a CCD camera for measuring small angle x-ray scattering. At the bottom right is the goniometer head that was used in this experiment to provide radial scanning of the flame (Y direction). The microscope head (black object) was not used.

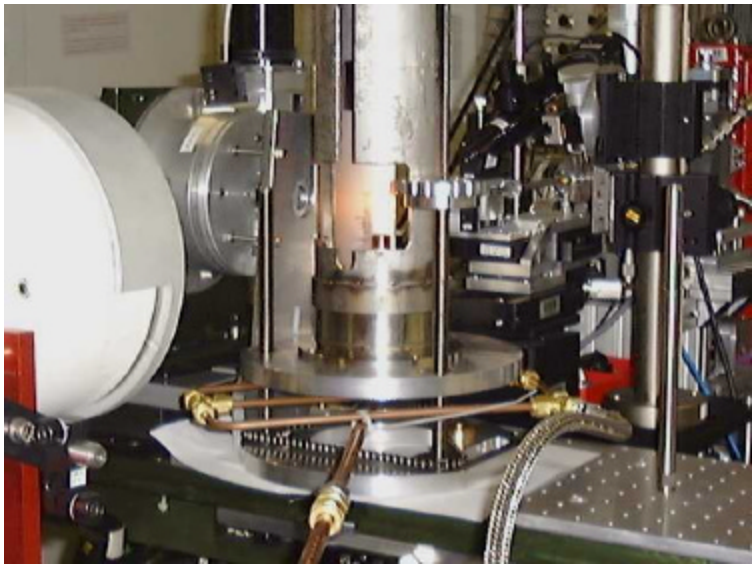

Fig. 10. This photograph shows another view of the experimental arrangement with the burner in place and the flame burning. The copper pipes feed fuel and air to the burner which is pushed and pulled in a horizontal direction by the goniometer head (silver object, left of center). The CCD camera is on the left (white object). The burner can be moved vertically manually.

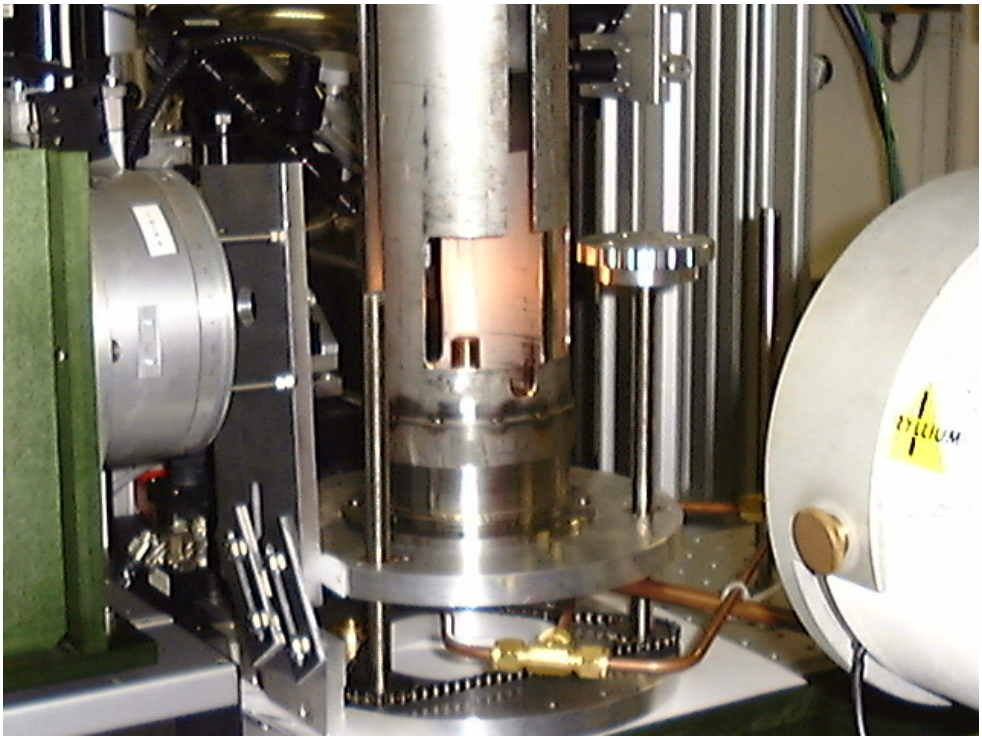

Fig. 11. This shows a view from the other side with the goniometer (on the left), the CCD camera (on the right) and the flame and mounting assembly (in the center).

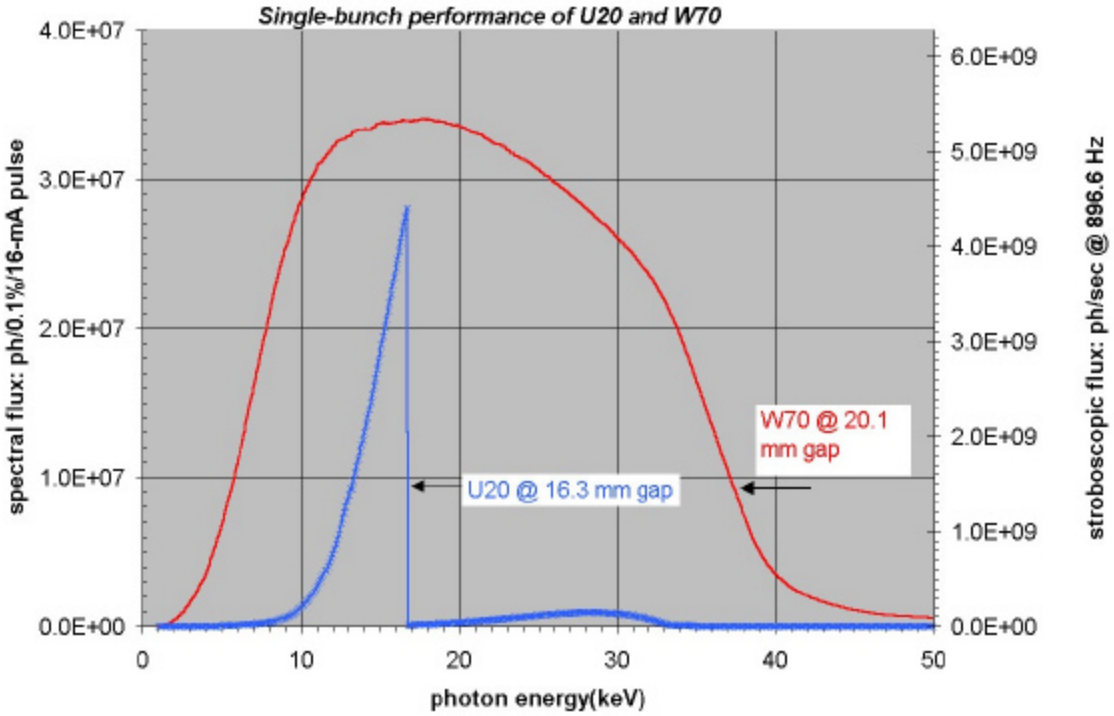

Fig. 12. The spectrum of x-rays coming from the undulators feeding the ID09 beamline. The W70 undulator was used for this experiment.

The present measurement represents a proof-of-principle experiment and it has to be said that the results were very satisfying and exceeded expectations. In the early analysis of expected signals, it was expected that ionization of soot particles by the x-ray beam would give rise to charged particle production rates comparable or less than those produced by natural ionization processes in the flame. Use of a lock-in amplifier was expected to be required in order to separate out x-ray induced signals from natural ionization signals. In fact we have found that the ionization rate under the beam conditions used, exceeded the natural flame ionization rate and so signals could be acquired directly. A simple cylindrical electrode, 1 mm in diameter and 50 mm long was used to collect the positively charged particles (ions, positive soot particles) when biased negatively or negative particles (electrons, negative ions, negative soot particles) when biased positively. The signals acquired were also larger than the background gas ionization which was not minimized in the experiment by reducing the pressure in the vicinity of the flame nor by shortening the exposure length.

Figure 13 shows the positive and negative ionization currents measured when the x-ray beam intersected the flame at a height of 32 mm above the burner throat. It can be seen that the x-ray induced signal is about a factor of ten larger than the background gas ionization rate. Figure 14 shows a similar plot but taken 2 mm above the burner throat. In this case there is no signal generated due to x-ray ionization of soot particles and this is to be expected from other studies. The curve labeled photodetector is a reading taken on a detector, located upstream in the x-ray beamline. This is normally use to yield a measure of the beam flux but it was found that when the flame was on, it yielded a much larger current which was due to light pickup from the flame. This proved to be useful as it provided a measure of the radial extent of the visible flame. For all the measurements taken at the synchrotron, a fuel flow rate of 62 ml/min of ethylene and 39 l/min of air yielding a flame with a height of 40 mm.

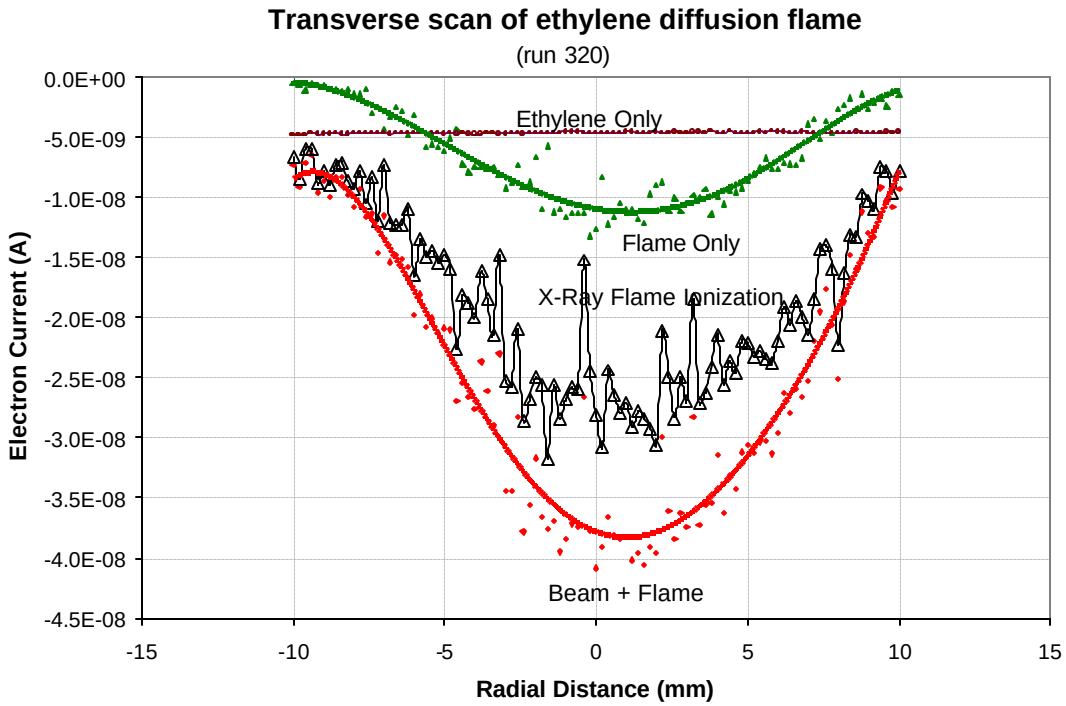

Fig. 13a Negative current received by probe at a height of 32 mm above burner (HAB)

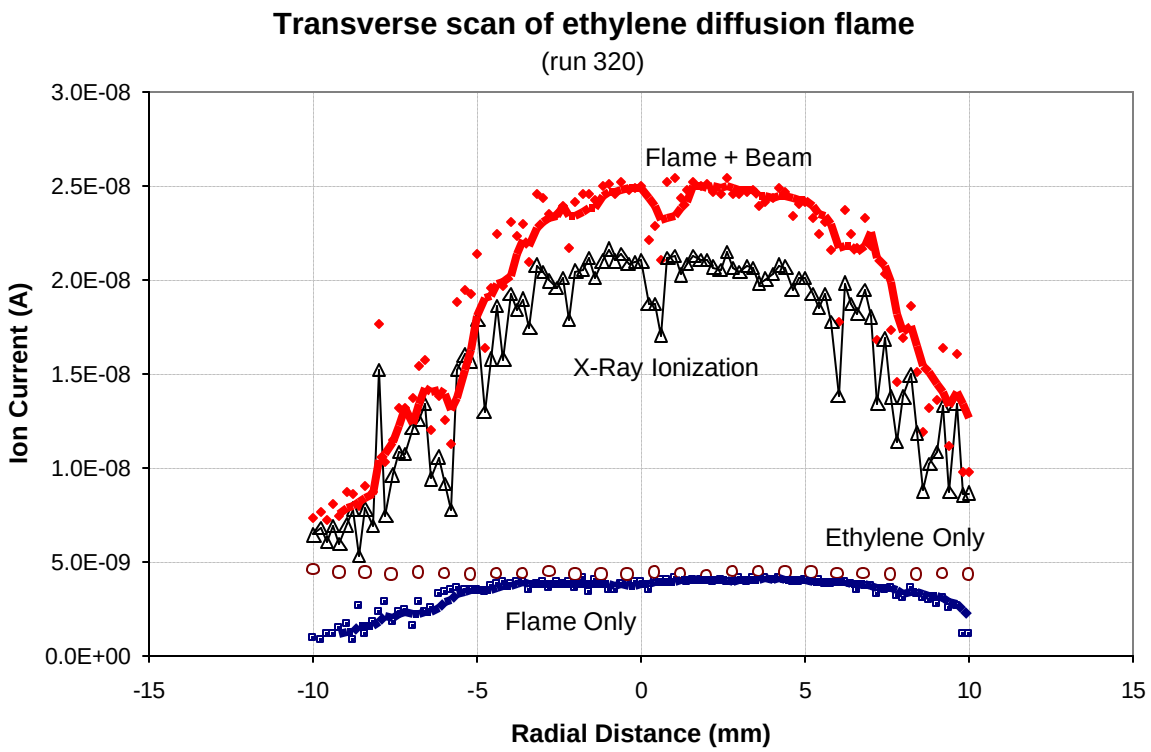

Fig. 13b. Positive charges received by the probe at a height of 32 mm above burner.

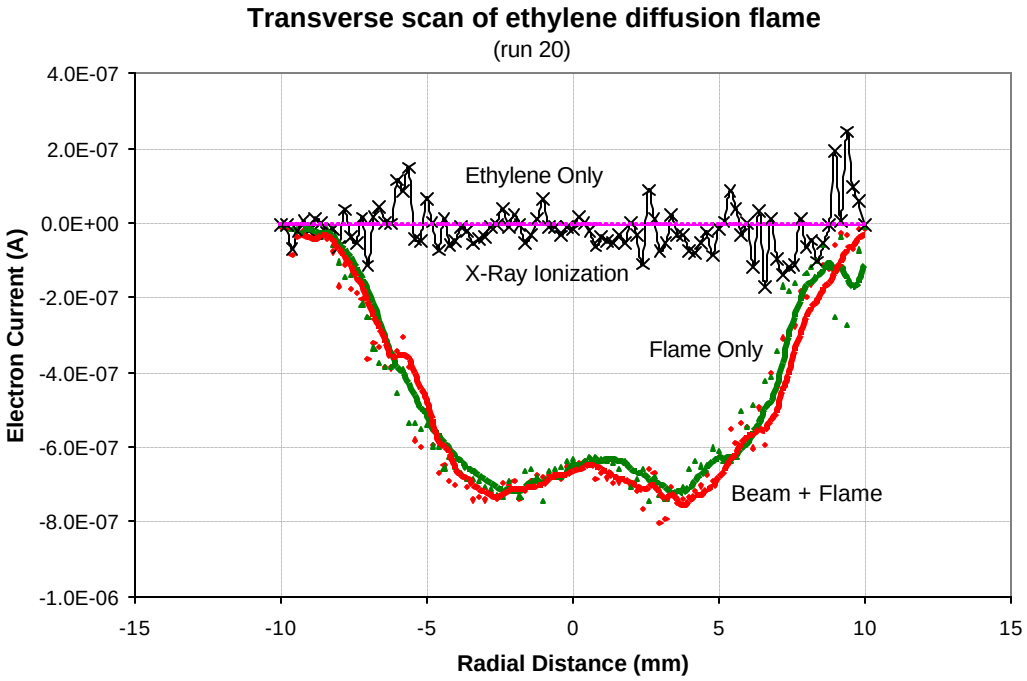

Fig. 14a. Negative charges received by the probe at a height of 2 mm above burner.

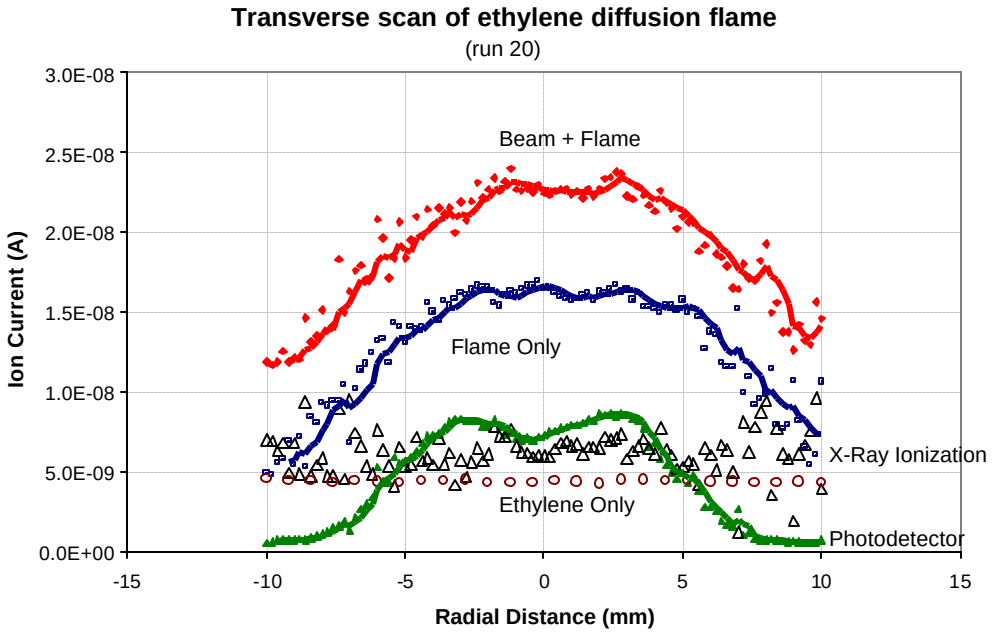

Fig. 14b. Positive charges received by the probe at a height of 2 mm above burner.

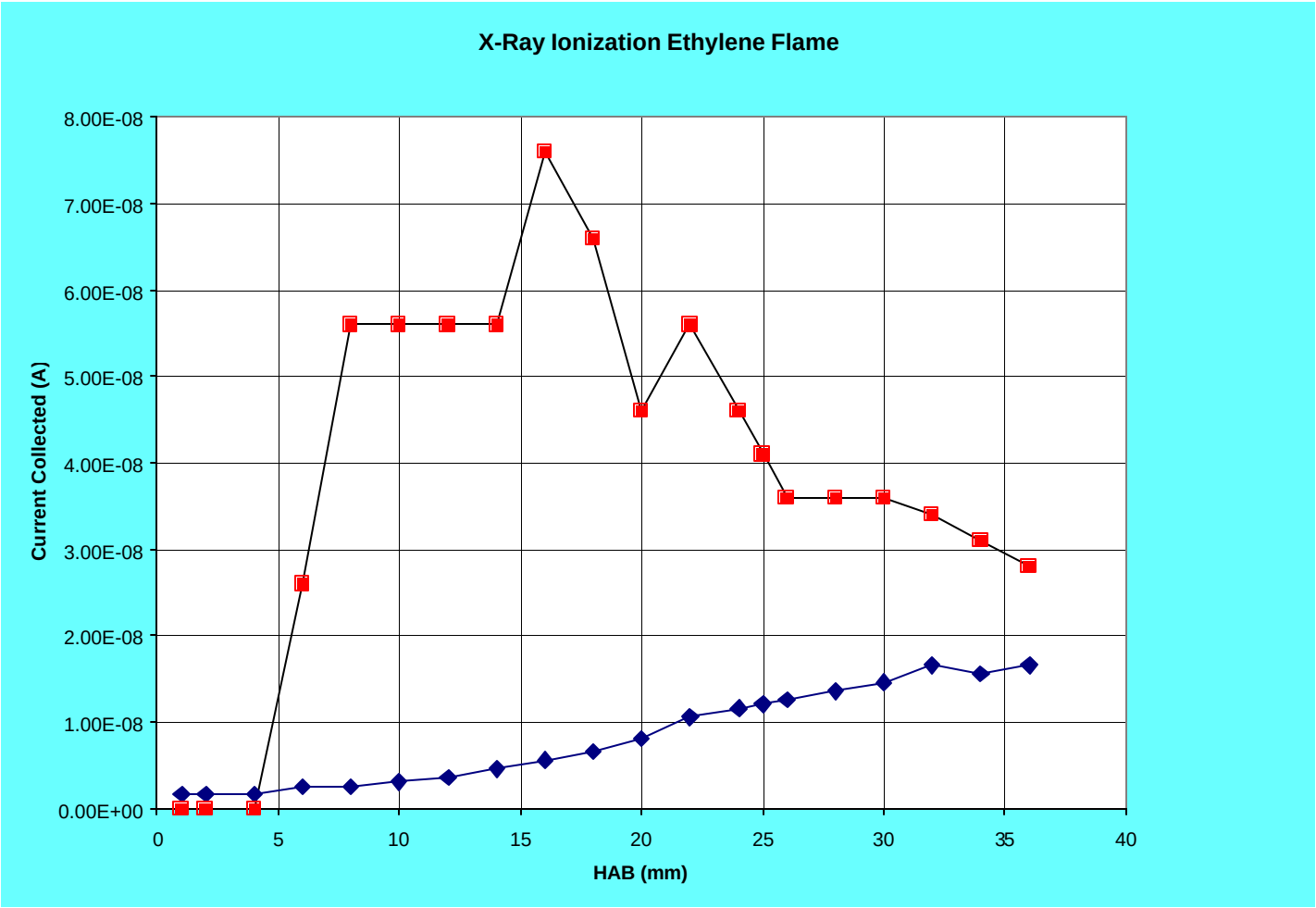

Fig. 15. Plot of positive and negative currents collected at burner center as a function of height above burner (HAB)

Figure 15 shows a plot of centerline ionization intensities plotted as a function of height above the burner. It can be seen that the positive ion current starts out constant up to around 10 mm whereupon it begins to rise, reaching a maximum at around 35 mm. The negative current, referred to as the electron current is seen to rise to a maximum at between 15 and 20 mm and then to fall off thereafter.

The cylindrical wire probe used to collect the charges acts somewhat like a conventional Langmuir probe but at atmospheric pressure, the collected currents never achieve saturation as occurs for low pressure probes. The reason for this is that while at low pressures, charges move towards a biased wire probe via diffusion across a sheath region

where the charge is unipolar, in the case of a high pressure probe, charges are convected towards the collector and the sheath region is very thin. This condition has been studied theoretically by Clements and Smy [35] who set down an equation relating the charge density and the measured current as follows:

$$I = 5.3\varepsilon_0^{1/4}\mu^{1/4}r_p^{1/4}e^{3/4}v_f^{3/4}n^{3/4}V^{1/2}l \quad \text{.....(2)}$$

where ε_0 is the permittivity of free space, e, the electronic charge, μ the mobility of the charged particle, n, the density of charged particles, V the applied probe potential, r_p and l, the radius and length of the probe. In the current measurement, r_p = 0.5 mm, l = 6 cm, and the potential applied to the probe was ± 22 V. Measurements by Santoro et al. [36] have shown that in an ethylene flame, the velocity varies from a value close to the initial fuel velocity (1 cm/s) to about 1.5 m/s at a height of 20 mm above the burner. This rapid acceleration is due to buoyancy and thermal expansion effects. Inserting these factors into equation (2) along with the physical constants yields:

$$I = 4.1x10^{-12}\mu^{1/4}n^{3/4} \quad \text{.....(3)}$$

It is seen that for a given charged particle density, the current is proportional to the (mobility)$^{1/4}$. Thus free electrons, released from the soot particles will yield larger measured currents that the heavy positive species left behind. This explains the larger negative currents measured in the region between 5 and 35 mm. The fact that the electron current declines between 20 and 35 mm, eventually reaching a value equal to the positive current, (that has been constantly rising over this range) suggests that free electrons attach to neutral soot particles and thus the mobility of the negative charge carriers drops sharply. In a subsequent experiment, the time structure of the synchrotron beam will be exploited to make actual measurements of the charged particle mobilities. This will greatly aid in their identification.

The fact that such large signals arising from x-ray absorption by soot particles were seen is very significant for it indicates that the physical processes occurring as a result of the absorption are complex. For high energy x-rays interacting with matter, the absorption cross section can be taken to be the sum of the photoionization cross sections for all the various subshells of the target atoms and the atoms constituting the material through which the x-ray passes are assumed to be independent. Table I lists the cross sections for carbon, oxygen and nitrogen atoms for energies of 10 and 20 keV.

Element	σ(10 keV) cm^2	σ(20 keV) cm^2
Carbon	4.12×10^{-23}	4.1×10^{-24}
Oxygen	1.48×10^{-22}	1.57×10^{-23}
Nitrogen	7.9×10^{-23}	8.27×10^{-24}

The cross section for the photoabsorption of air by a 20 keV x-ray photon is therefore 1×10^{-23} cm^2. Using Beer's law, one can calculate the number of photoionization events per incident photon (I/I_{0}) thus:

$I/I_0 = nl\sigma = 2 \times 3.2 \times 10^{16} \times 760 \times 6 \times 1 \times 10^{-23}$

where n is the number density of target atoms. (3.2×10^{16} molecules per Torr, 1 atm = 760 Torr). Collection length 6 cm.

Thus $I = 2.4 \times 10^{-3} I_0$

From figure 4 we see that the soot volume fraction is of the order of 4 x 10^{-6} at 32 mm height, the density of soot particles is 2.2 gm/cm^3 and the molecular weight of carbon is 12. Thus using Avogadro's number, the number density of carbon atoms in the target soot is seen to be:

$$n_{carbon} = \frac{2.2 x 4 x 10^{-6} x 6 x 10^{23}}{12} = 4.4 x\ 10^{17}\ cm^{-3}$$

and so :

$I = I_0 \times 4.4 \times 10^{17} \times 1 \times 4.1 \times 10^{-24} = 1.8 \times 10^{-6}\ I_0$

where the optical depth in the flame is approximately 1 cm. Thus the number of ionization events due to soot absorption should be of the order of 100 times less than that produced by the background gas. Despite this, as clearly seen in figure 13, the absorption of x-rays in the flame yields a signal about ten times greater than that due to background gas ionization. This is a very interesting and significant result.

The reason for this discrepancy can be explained by considering the photoemission yield from soot particles as compared with air molecules. When a molecule of oxygen or nitrogen absorbs a high energy x-ray, an inner shell electron is ejected creating an inner shell vacancy. An electron from a higher shell may drop down into the vacancy thus emitting a photon (i.e fluorescence) or the energy thus released may be carried away by the emission of another electron. This process is known as the Auger effect. Thus more than one electron may be produced by the photoabsorption event. In a solid particle, the situation is much more complex for one can have a cascade of auger electrons produced and the energetic electrons thus released may subsequently ionize other atoms in the material. In this way many electrons can be produced by a single high energy x-ray photoabsorption event. The loss of a number of electrons from a small particle leads to the generation of extremely high electric fields that

can cause field emission of electrons and also disruption and fragmentation of the particle. Thus the whole photoabsorption process is an extremely violent event.

These processes have been discussed in a number of astrophysical papers [21-26] as the absorption of x-rays by interstellar dust is an important issue in observational astronomy. Up to now there has been no experimental data to support or to confront these models. Clearly a lot more study and experimentation is required before a proper understanding of this phenomenon is acquired and before the interpretation of the signals can be properly applied in a combustion or an astrophysical environment. In the next series of experiments, planned for the synchrotron, it is intended to use a premixed flame as a target and to house the flame in a cryogenically pumped vacuum chamber. This will allow a cleaner measurement to be performed. It will also permit longer wavelength photons (VUV) to be used. By exploiting the time structure of the synchrotron radiation, the mobilities of the collected particles can be determined and this will provide more information concerning fragmentation and processes as well as electron attachment processes in the flame. It will also be very instructive to study absorption at other wavelengths and in particular in the ultra-violet region.

ACKNOWLEDGEMENTS

The financial support of the European Office of Aerospace Research and Development, Air Force Office of Scientific Research, Air Force Research Laboratory and the continued encouragement and interest of Dr. Charbel Raffoul is gratefully acknowledged. Gratitude is also due to the European Synchrotron Radiation Facility and in particular to Dr. Michael Wulff for the provision of their facilities and scientific support in the x-ray

absorption measurements. Thanks are also due to the technical skills of M. Daniel Travers and M. René Jaffre of the University of Rennes for the construction of the apparatus.

REFERENCES

1. Choi, M.Y., Mulholland, G.W., Hamins, A. and Kashiwagi, T.

   Comparison of the soot volume fraction using gravimetric and light extinction techniques.

   Combustion and Flame **102,** 161-169, 1995.

2. Santoro, R.J., Semerjian, H.G. and Dobbins, R.A.

   Soot particle measurements in diffusion flames

   Combustion and Flame, **51**, 203, 1983.

3. Vander Wal, R.L. and Weiland, K.J.

   Laser induced incandescence – development and characterization towards a measurement of soot volume fraction

   Appl. Phys. B. Lasers and Optics **59**, 445-452, 1994.

4. Vander Wal, R. Jensen, K.A. and Choi, M.Y.

   Simultaneous laser induced emission of soot and polycyclic aromatic hydrocarbons within a gas jet diffusion flame

   Combustion and Flame **109**, 399-414, 1997.

5. D'Alessio, A. D'Anna, A., Gambi, G. and Minutolo, P.

   The spectroscopic characterization of UV absorbing nanoparticles in fuel rich soot forming flames

   J.Aerosol. Sci. **29**, 397-409, 1998.

6. Smyth, K.C. and Mallard, W.G.

   Laser induced ionization and mobility measurements of very small particles in premixed flames at the sooting limit

   Combustion Sci. Tech. **26**, 35-41, 1981.

7. De Iulius, D., Barbini, M., Benecchi, S., Cignoli, F. and Zizak, G.

Determination of the soot volume fraction in an ethylene diffusion flame by multiwavelength analysis of soot radiation

Combustion and Flame **115**, 253-261, 1998.

8. Dobbins, R.A. and Megaridis, C.M.

Morphology of flame generated soot as determined by thermophoretic sampling

Langmuir, **3**, 254-259, 1987.

9. Hepp, H. and Siegmann, K.

Mapping of soot particles in a weakly sooting diffusion flame by aerosol techniques

Combustion and Flame **115**, 275-283, 1998.

10. Saito, K., Gordon, A.S. Williams, F.A. and Streibel, T.

A study of the early history of soot formation in various hydrocarbon diffusion flames

Combustion Sci. Tech. **80**, 103, 1991.

11. Vander Wal, R.

A TEM methodology for the study of soot particle structure

Combustion Sci. Tech. **126**, 333-357, 1997.

12. Vander Wal, R.

Soot precursor carbonization: vizualization using LIF and LII and comparison using bright and dark field TEM.

Combustion and Flame **112**, 607-616, 1998.

13. Ishiguro, T., Takatori, Y and Akihama, K.

Microstructure of diesel soot particles probed by electron microscopy: first observation of inner core and outer shell.

Combustion and Flame **108**, 231-234, 1997.

14. Dobbins, R.A., Govatzidakis, G.J., Lu, W., Schwartzmann, A.F. and Fletcher, R.A.

Carbonization rate of soot precursor particles

Combustion Sci. Tech. **121**, 103-121, 1996.

15. Majidi, V., Saito, K., Gordon, A.S. and Williams, F.A.

Laser desorption time-of-flight mass-spectrometry analysis of soot from various hydrocarbon fuels

Combustion Sci. Tech. **145**, 37-56, 1999.

16. Reilly, P.T.A., Gieray, R.A., Whitten, W.B. and Ramsey, J.M.

Direct observation of the evoluation of the soot carbonization process in an acetylene diffusion flame via real time aerosol mass spectrometry

Combustion and Flame **122**, 90-104, 2000.

17. Weilmunster, P, Keller, A. and Homann, K.H.

Large Molecules, radical ions, and small soot particles in fuel rich hydrocarbon flames, part I: Positive ions of polycyclic aromatic hydrocarbons (PAH) in low pressure premixed flames of acetylene and oxygen.

Combustion and Flame **116**, 62-83, 1999.

18. Puri, R., Santoro, R.J. and Smyth, K.C.

The oxidation of soot and carbon monoxide in hydrocarbon diffusion flames

Combustion and Flame **97**, 125-144, 1994.

19. Pratsinis, S.E.

Flame Aerosol Synthesis of ceramic powders

Prog. Energy Combust. Sci. **24**, 197-219, 1998.

20. Wooldridge, M.S.

Gas Phase Combustion Synthesis of Particles

Prog. Energy Combust. Sci. **24**, 63-87, 1998

21. B.T. Draine and E.E. Salpeter

On the physics of dust grains in hot gas

Astrophys. J. **231**, 77-94, 1979.

22. C.A. Chang, A.V.R. Schiano and A.M. Wolfe

The Effect of a quasi-stellar object on its host galaxy: Dynamical and physical processes in the interstellar medium around a quasi-stellar object.

Astrophys. J. **322**, 180-200, 1987.

23. G.M. Voit

X-ray irradiation of interstellar grains in active galaxies: evaporation and infrared spectra.

Astrophys. J. **379**, 122-140, 1991

24. G.M. Voit

Destruction and survival of polycyclic aromatic hydrocarbons in active galaxies

Mon. Not. R. Astron. Soc. **258**, 841-848, 1992.

25. A. Laor and B.T. Draine

Spectroscopic constraints on the properties of dust in active galactic nuclei

Astrophys. J. **402**, 441-468, 1993

26. E. Dwek and R.K. Smith

Energy deposition and photoelectric emission from the interaction of 10 eV to 1 MeV photons with interstellar dust particles

Astrophys. J. **459**, 686-700, 1996.

27. Dasch, C.J.

One dimensional tomography: a comparison of Abel, onion-peeling, and filtered backprojection methods.

Applied Optics **31**, 1146-1152, 1992.

28. Santoro, R.J., Semerjian, H.G., Emmerman, P.J. and Goulard, R.

Optical Tomography for Flow Field Diagnostics

Int. J. Heat Mass Transfer **24**, 1139-1150, 1981.

29. Hayhurst, A.N. and Jones, H.R.N.

J. Chem. Phys. Faraday Trans. **83**, 1, 1987.

30. Goodings, J.M., Tanner, S.D. and Bohme, D.K

Can. J. Chem. **60**, 2766, 1982.

31. Keil, D.G. Gill, R.J., Olson, D.B. and Calcote, H.F. in *The Chemistry of Combustion Processes* (ed. T.F. Sloane) American Chem. Soc. Washington DC, 1984, p. 33.

32. Gerhardt, Ph. and Homann, K.H.

J. Chem. Phys. **94**, 5381, 1990.

33. Gerhardt, Ph. and Homann, K.H.

Ber. Bundenges. Phys. Chem. **94**, 1086, 1990.

33. Fialkov, A.B.

Investigations on ions in flames
Prog. Energy Combust. Sci. **23**, 399-528, 1997.

34. Calcote, H.F.

Mechanisms of soot nucleation in flames – a critical review

Combustion and Flame **42**, 215-242, 1981

35. Clements, R.M. and Smy, P.R.

J. Appl. Phys. **41**, 3745, 1970.

36. Santoro, R.J., Yeh, T.T., Horvath, J.J. and Semerjian, H.G.

The transport and growth of soot particles in laminar diffusion flames

Combustion Sci. Tech. **53**, 89-115, 1987.

APPENDIX

Experimental Team at ESRF Synchrotron Experiment

Team Leader: Prof. J. Brian A. Mitchell - U. Rennes

Prof. C. Rebrion-Rowe - U. Rennes

Dr. J.L. LeGarrec - U. Rennes

G. Taupier - U. Rennes

N. Huby - U. Rennes

Beamline Scientist: Dr. Michael Wulff - ESRF